C-FD MAC : Constellation Based Full-Duplex MAC protocol

PROJECT REPORT

Submitted by

SURYA BHUSHAN DWIVEDI

in partial fulfillment of the requirements

for the award of the degree of

MASTER OF TECHNOLOGY

Department Of Electrical Engineering

INDIAN INSTITUTE OF TECHNOLOGY MADRAS

MAY 2022

DEPARTMENT OF ELECTRICAL ENGINEERING

INDIAN INSTITUTE OF TECHNOLOGY MADRAS

2022

CERTIFICATE

This is to certify that this thesis (or project report) entitled ***"C-FD MAC : Constellation Based Full-Duplex MAC protocol"*** submitted by **Surya Bhushan Dwivedi** to the Indian Institute of Technology Madras, for the award of the degree of **Masters of Technology** is a bona fide record of the research work done by him under my supervision. The contents of this thesis (or project report), in full or in parts, have not been submitted to any other Institute or University for the award of any degree or diploma..

Dr. T. G. Venkatesh
Research Guide
Associate Professor
Department of Electrical Engineering
IIT Madras 600036

Acknowledgment

First and foremost, I would like to express my deepest gratitude to my guide, **Dr. T.G Venkatesh**, Associate Professor, Department of Electrical Engineering, IIT Madras, for providing me an opportunity to work under him. I would like to express my deepest appreciation for his patience, valuable feedbacks, suggestions and motivations.

I convey my sincere gratitude to Ankit Kumar Gupta, PhD Scholar, IIT Madras, for all his suggestions and support during the entire course of the project. Throughout the course of the project he offered immense help and provided valuable suggestions which helped me in completing this project.

I would like to extend my appreciation to all my friends and for their help and support in completing my project successfully.

Abstract

Many communications techniques have been developed in recent years to improve system throughput. Full-Duplex (FD) communication is one of those approaches. Transmission and reception of data packets at the same frequency is not possible in Half Duplex (HD) communication; but, simultaneous transmission and reception of data packets is possible in Full-Duplex (FD) communication, which is why FD can theoretically double system throughput. Effective self-interference (SI) cancellation is necessary in the case of symmetrical links, and additional inter node interference (INI) cancellation is required in the case of asymmetrical links, to fully use FD communication in realistic circumstances. Due to these difficulties, a good symbol decoding method is also necessary at the receiver end. For wireless local area networks (WLAN) a constellation-based FD medium access control (MAC) protocol (C-FD) is proposed in this report. The proposed C-FD MAC protocol allows the node and Access Point (AP) to exchange packets at the same time by broadcasting symbols using various modulation schemes . At both ends, the superimposed constellation diagram was employed to efficiently decode the symbols. Here superposition of constellation diagram meant by superposition of constellation diagrams used by node's Tx and AP's Tx. The C-FD MAC protocol is unique in that it does not necessitate the use of sophisticated interference cancelling techniques like SI cancellation techniques in symmetrical and asymmetrical link or INI cancellation techniques in asymmetrical link . For the symmetrical and asymmetrical FD links, analytical results for Symbol Error Rate (SER), Packet Error Rate (PER) and throughput have been derived using the additive white gaussian noise (AWGN) channel. When compared to Half duplex (HD) transmission, the proposed C-FD MAC protocol achieves double the throughput without sacrificing the SER. The Markov chain model for RTS transmission is aimed to prove that transmission of the RTS is achievable when the backoff counter is zero. The RTS collision probability is calculated here using the Markov chain model. Extensive simulation was used to validate the analytical results.

Contents

List of Figures

List of Tables

ABBREVIATIONS

AP	Access Point
AWGN	Additive White Gaussian Noise
BPSK	Binary Phase Shift Keying
C-FD	Constellation-based Full- Duplex
CSI	Channel State Information
CTS	Clear To Send
DCF	Distributed Coordination Function
FD	Full Duplex
FDD	Frequency domain duplexing
HD	Half Duplex
INI	Inter Node Interference
MAC	Medium Access Protoco

MTS	Modulation and Coding Schem
M-PAM	M-ary Pulse Amplitude Modulation
m-PSK	m-ary Pulse Shift Keying
PER	Packet Error Rat
QPSK	Quadrature Phase Shift Keying
RSI	Residual Self Interference
RTS	Request To Send
SER	Symbol Error Rate
SNR	Signal to Noise Ratio
TDD	Time domain duplexing
WLAN	Wireless Local Area Network

Chapter 1

Introduction

As we know that the users of mobile devices are increasing dramatically over the last few decade. It is common for data to be accessed via cloud services rather than being physically stored on the device. Furthermore, video and audio streaming data services become very popular now a days which are increasing data traffic rapidly. Development of faster wireless communication systems got acceleration due to this. Now a days so many new wireless communication techniques are evolving but these are reaching to their theoretical limits.

In the electromagnetic spectrum, all radio systems which are available for communication require a fixed bandwidth. Regulation of the radio spectrum done very heavily by governments. A large portion of the radio spectrum has been set aside for uses other than wireless mobile communications. As a result, it is critical to make the best use of the limited spectrum available. The rate at which information can be communicated over a given bandwidth is referred to as spectral efficiency. Transmission and reception are separated in time or frequency in traditional wireless communication systems, which are known as time domain duplexing (TDD) and frequency domain duplexing (FDD), respectively. However, it is obvious that a system capable of transmitting and receiving on the same frequency simultaneously

would double the spectral efficiency. This is known as in-band full-duplex.

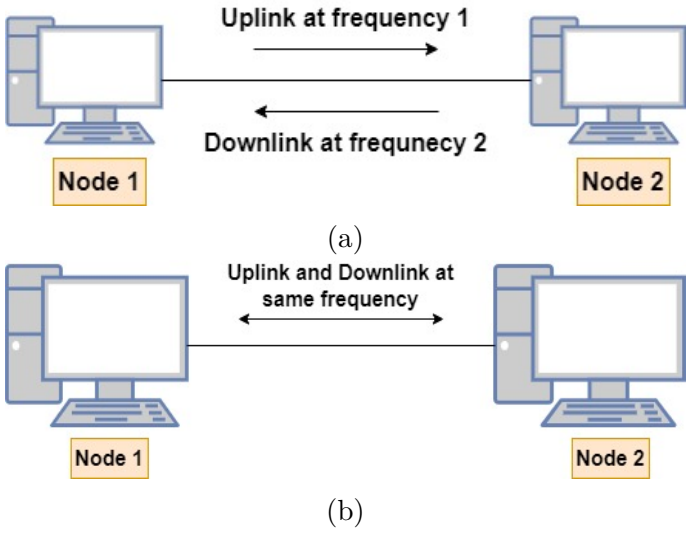

Figure 1.1: (a) Half Duplex (b) Full Duplex

Half Duplex (HD) communication is created when upink (UL) data transmission occurs from Node 1 to Node 2 at one frequency and downlink (DL) transmission occurs from Node 2 to Node 1 at another frequency, as seen in fig 1.1a. Full-Duplex (FD) communication occurs when UL transmissions from Node 1 to Node 2 and DL transmission from Node 2 to Node 1 occur at the same frequency as seen in fig 1.1b.

FD communication has the potential to satisfy the rising data traffic demand while also lowering latency. FD communication has the potential to double the spectral efficiency of existing Wireless Local Area Network (WLAN) systems [1]. FD communication has several advantages, including increased throughput, reduced collision, reduced end-to-end time, and the avoidance of the hidden node problem [2]. We must overcome major hurdles such as Self Interference (SI), imprecise interference cancellation, increased power consumption, and hardware complexity to obtain the stated benefits of FD communication [3]. SI can be suppressed up to 110 dB by combining analogue and digital domain cancellation and bringing the SI to the noise level, according to recent research [4]. However, even with modern approaches,

perfect SI cancellation is not possible, resulting in FD communication system performance degradation [5].

The SI component is substantially stronger than the desired signal at the receiver end in FD communication. To minimise the SI, expensive and sophisticated analogue and digital circuitry are required [6]. In practise, the incomplete cancellation at the receiver end causes Residual Self Interference (RSI) [7]. Constellation-based symbol decoding algorithms, on the other hand, have previously been used and provide outstanding performance in Half-Duplex (HD) communication with less complexity [8]. The superposition technique was first introduced for the Additive White Gaussian Noise (AWGN) channel by T. M. Cover in [9]. The fundamental goal of superposition coding is to send two or more data over a noisy channel by combining them into a single data stream and decoding the superimposed data at the receiver. For multi-user data transfer, numerous superposition encoding strategies and efficient decoding algorithms to retrieve the encoded packet have been suggested [10], [11], [12]. In the existing literature, however, no constellation-based symbol decoding or superposition encoding technique has been developed to alleviate SI and facilitate FD communication.

As previously stated, SI has a significant impact on the received signal in both symmetrical and asymmetrical networks. Inter node interference (INI) becomes stronger in an asymmetrical link when both nodes are within range of each other. INI will not be present if both nodes are not in the same range.

This report's major purpose is to offer an efficient constellation-based symbol decoding algorithm for FD communication that does not need SI cancellation. We also propose a Constellation-based Full-Duplex (C-FD) MAC protocol that incorporates the above method. The following are the innovative aspects of our proposed C-FD MAC protocol. It operates even in the worst-case scenario, where the entire signal power is lost from the transmitter to the receiver (node or AP). To put it another way, our suggested C-FD MAC protocol works with standard two-antenna devices without suppressing self-interference.

The C-FD algorithm operates as follows in a nutshell. The node and the AP

both send out symbols at the same time, but with distinct modulation schemes and power levels. Symbol decoding at the AP and node can be done by computing the maximal likelihood conditional probability at the receiver end using the constellation diagram of the interfering signals.

1.1 Outline Of Report

The first chapter provides a brief overview of contemporary communication difficulties, how FD communication fits into the picture, challenges in creating FD communication, and an overview of the proposed work.

In the second chapter, theory and background on in-band full duplex, self interference cancellation techniques, and modulation techniques are discussed. This section concludes with our unique contribution. In first section, in band full duplex theory and Full Duplex's applications are mentioned like doubling the capacity, used in base stations and creating the Medium access protocol. In second section, self interference cancellation techniques are addressed in three domains: the RF domain, the analog domain, and the digital domain. In third section, modulation techniques related works used in FD communication is discussed.

System modelling, our proposed constellation-based Full Duplex MAC protocol and a symbol decoding technique for our proposed MAC protocol is discussed in the third chapter. The development of links in FD communication is covered in the first section. In FD communication, there are two forms of link formation: symmetrical link and asymmetrical link. In this chapter, both are thoroughly discussed. Following that, we cover how we create constellation diagrams on the Tx side of nodes and APs, as well as how we use these Tx constellation diagrams on the Rx side of the AP and nodes in our proposed work. Our proposed constellation-based Full Duplex MAC protocol is explained in the second section. We discussed about RTS/CTS transmission as well as packet transmission from the AP to the nodes and the nodes to the AP in this chapter. In the third section, we provide a symbol

decoding technique for our proposed MAC protocol. We discussed symbol decoding algorithms for both symmetric and asymmetric links in this section.

All analytical derivations are added in the fourth chapter. First, we calculated the proposed C-FD MAC protocol's Symbol error rate (SER). In both symmetrical and asymmetrical links, we find SER at the node and AP. We also used SER to calculate Packet Error Rate (PER) for both symmetrical and asymmetrical links. The RTS collision probability for our proposed C-FD MAC protocol was then calculated. Using PER and RTS collision probability, we calculated throughput for our proposed C-FD MAC protocol.

In the fifth chapter, we used simulation results to verify all of the analytical derivations. For our proposed C-FD MAC protocol, we used MATLAB 2021a software to display simulation graphs for SER, PER, RTS collision probability, and Throughput.

In the final chapter, we summarised our work and stated that we had achieved all of our desired goals in C-FD MAC protocol.

Chapter 2

Theory and Background

We covered the theory of in-band full duplex, self-interference cancellation techniques in this chapter. Later, we described the background work that had been done in this subject up to that point, including modulation techniques, because modulation techniques played a vital part in achieving the desired result in this study. The first portion also includes FD's applications. The second section discusses three types of SI cancelling techniques: RF, analog, and digital domain. In the final section of this study, we highlighted our distinctive contribution.

2.1 In band Full Duplex

Various methods of performing bidirectional communication across a common channel are referred to as duplexing. FDD and TDD are two common RF communication technologies. Transmission and receiver signals are separated into two different frequency channels in FDD. TDD uses at a time one frequency channel and can only broadcast or receive at the same time. A common application of TDD is

the wireless local area network (WLAN). Because transmission and decoding of signal do not occur concurrently on the same channel, FDD and TDD are half-duplex systems. In-band full duplex (also known as full duplex (FD)) employs only one channel to perform uplink and downlink data transmission simultaneously. Figure 2.1 depicts the differences between the three duplexing approaches. The spectral efficiency of full-duplex would theoretically double. The needed frequency bands would be halved in comparison to FDD, and the efficiency of the specific frequency channel would be theoretically doubled in comparison to TDD.

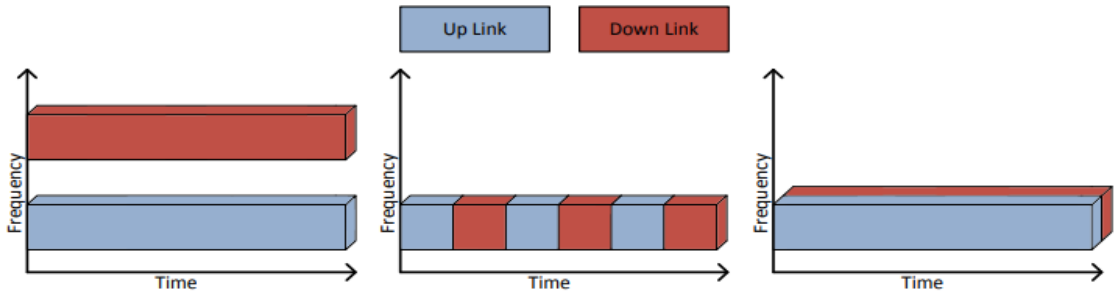

Figure 2.1: From left to right: FDD, TDD and FD.

The SI, or unintended coupling of the system's own transmission (TX) signal to the reception (RX) signal, is a drawback of full-duplex. Non-ideal isolation between the transmitter and receiver causes the SI. The signal-of-interest (SoI), which contains the data to be received, can be almost 90 dB more intense than the typical TX signal. Even though the SI is naturally attenuated, the signal strengths still differ significantly. Under SI from the TX signal, the SoI is lost. The SI must be greatly lowered in order to make the SoI signal observable again. Simply put, the SoI is created by subtracting the TX signal from the RX signal. Both analogue and digital domains are used for SI cancellation.The goal of analog cancellation is to reduce the SI's power so that the receiver's dynamic range can cover both the SI and the SoI. The remaining SI is digitally cancelled.

2.2 Applications of Full Duplex

There are helpful applications mentioned in this part, in addition to the immediate and most prolific advantage of IBFD to double the link capacity.

2.2.1 Doubling the Capacity

If both nodes are IBFD in bidirectional wireless data transmission, the link capacity can possibly be doubled, assuming perfect SIC. This may not always be the case. However, a significant amount of SIC can be obtained in practise. Thus, capacity improvements are recorded that are less than twice, but still quite high, reaching 1.84 .

2.2.2 Base Stations

A base station (BS) in a multi-user network (such as cellular) serves several users. Making the BS IBFD alone can greatly expand the network. In base station topologies, it is preferable to place as much complexity and power consumption on the BS as feasible rather than on user equipment. As a result, only the BS is likely to be converted to full duplex. The key benefit is that the BS may simultaneously serve two customers with no additional time or frequency resources because the same frequency band can be used for both uplink and downlink to either user. Assuming that inter-user interference is controllable, this application can save the network operator money on commercial spectrum that is too expensive. Another, related application would be backhaul communications using the same frequency band .

2.2.3 Medium Access Control

The major advantage of employing IBFD at the medium access control (MAC) layer is that it solves the hidden node problem, which is common in carrier sense

multiple access networks. The hidden node problem can occur in a three-node one-hop network scenario in which only one node can contact both nodes but the other two nodes cannot reach each other directly, i.e. a line arrangement. The nodes that are unaware of (i.e. concealed from) each other can attempt to interact with the centre node, which has access to both, at the same time, resulting in a collision. In this scenario, if IBFD is only utilised for the middle node, the middle node can transmit a "busy" signal while receiving from either node, requiring the transmitting node to first listen for the "busy" signal and alter its transmission accordingly.

[3], [13] and [14] reviewed the Medium Access Protocol (MAC) supporting FullDuplex (FD) communication and its accompanying problems. Rukaiya et al. investigated the performance of a hybrid MAC protocol for FD ad-hoc networks that combines the advantages of TDM and IEEE 802.11 distributed coordination function (DCF) [15]. The asymmetric FD MAC technique with random back-off and carrier sensing was studied by Rama kiran et al. [16]. To fully exploit the channel access opportunities, Jingzhi Hu et al. presented a hybrid halfduplex(HD)/FD MAC protocol based on an RTS/CTS conflict resolution mechanism [17]. M. Omar Al-Kadri et al. suggested a distributed network energy-FDM MAC protocol [18]. To capture the channel in the energy-FDM MAC protocol, the RTS is broadcast with maximum power at the conclusion of the backoff timer.

2.3 Self Interference Cancellation

The three domains of self-interference cancellation are described in this section: RF domain, analog domain and digital domain. Their analysis is done individually and in groups.

2.3.1 RF SIC

The SI in an RF transmission can be cancelled in two ways. The passive and active SICs are both integrated into the RF SIC block illustrated in fig. 2.2.

Passive RF SIC

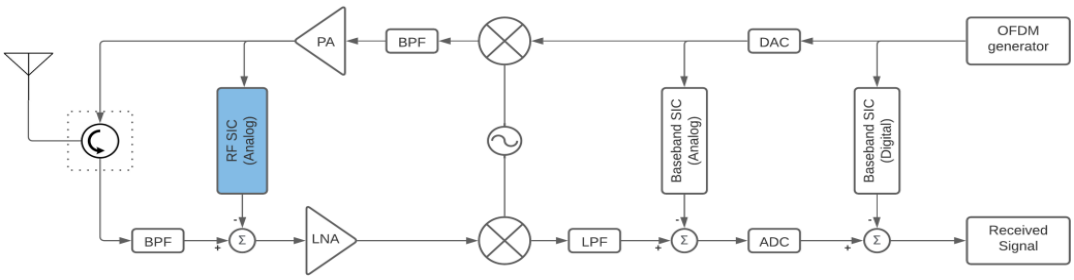

Figure 2.2: Block diagram for passive and active RF SIC

To attenuate the RF signal, the passive SIC employs a variety of approaches. In RF, a dual-polarized antenna can be used to cancel SI. The signal can be reduced by altering the polarisation of the antennas. In analogue RF, the simplest technique to attenuate the signal is to physically isolate or separate the transmitter and receiver. A circulator can be used with a transceiver. For the signal, a circulator acts as a one-way street. Allowing the transmitted signal to reach the antenna while blocking the signal from reaching the received signal chain. However, this isolation is not perfect, and in the receiver side of the signal chain, leakage of the sent signal is blended with the received signal. However, this isolation is not perfect, and in the receiver side of the signal chain, leakage of the sent signal is blended with the received signal.Dual polarised antennas may produce an average of 90dB SI isolation at 300GHz with a small antenna size.

The analog RF cancellation relies heavily on passive suppression. The line of sight radio signal between the transmit antenna and the receiving antenna is suppressed by isolating the transmitter from the receiver. In some circumstances, this

suppression can reach 70dB. A appropriate degree of RF SIC suppression is estimated to be around 20-40dB. The level of compression is determined by the bandwidth, centre frequency, and techniques employed.

Active RF SIC

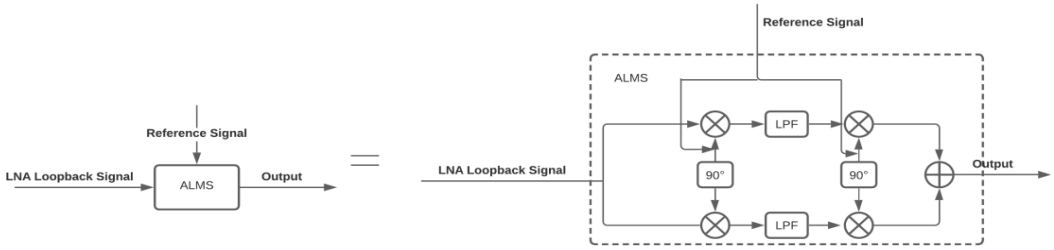

Figure 2.3: Block diagram for ALMS

The active RF SIC is required to attenuate the signal sufficiently to avoid SI saturation of the LNA and/or ADC. The signal would be corrupted and unintelligible if one of these were saturated. The Analog Least Mean Square (ALMS)adaptive filter developed in is one Analog SIC technique.

The ALMS multi-tap filter seen in Figure 2.3 processes the transmitted signal x(t) at various time delays, as $x(t - lT_d)$, where TD is the time delay and l is the number of time delays. In the ALMS shown in figure 2.18, the transmitted signal is combined with the LNA loopback signal.

2.3.2 Analog SIC

Researchers have attempted to add another analogue SIC to the base band. The analogue base band SIC, like the analogue RF SIC, is included to keep the ADC from being saturated. If the pass band cancellation isn't high enough, this is a key

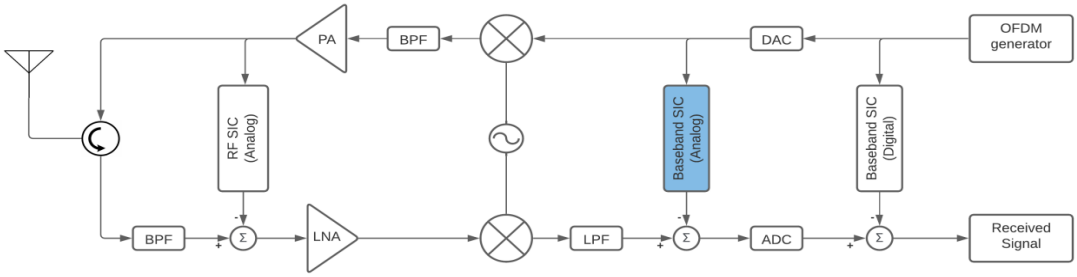

Figure 2.4: Block diagram for Analog SIC

step. To ensure that the ADC is not saturated, several critical considerations must be considered.

- Power of the received signal.
- Power of the SI.
- Cancellation in the passband.
- Number of bits in the ADC.

$$SINR = P_r - (P_{SI} - P_{ac}) \tag{2.3.1}$$

Equation 2.3.1 can be used to define the SINR after the LNA (assuming the LNA is not saturated), where Pr is the power of the received signal, PSI is the power of the SI, and Pac is the total analog cancellation in the passband.

2.3.3 Digital SIC

Because analog SICs are never perfect, residuals must be handled utilising digital SIC approaches. The digital cancellation is used to remove enough residuals from the signal so that it can be understood. Figure 2.5 depicts the digital SIC. The signal chain must be represented in order to cancel the signal in the digital domain. This necessitates the estimation of the system's transfer function. This is accomplished

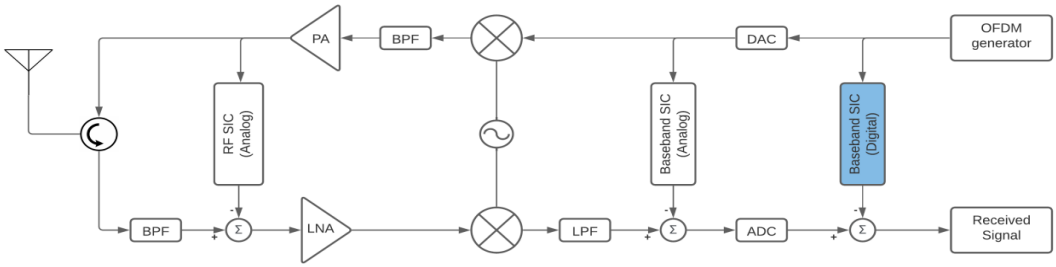

Figure 2.5: Block diagram for Digital SIC

by calculating the number of signal alterations and creating features to represent each of them. The filter should be trained to evaluate weights for each of these features after the features have been constructed. The filter estimates a portion of the entire signal to estimate weights, which are then subtracted from the signal together with their associated feature to ideally just export the received signal to the demodulator with no residuals.

The truth, however, is not as straightforward as the theory suggests. To avoid any delays, the digital filter must be fast enough. This indicates that the features must be optimised, and no further features should be added. Because the environment is always changing, the filter should be adaptable to modest changes over time. This implies that the filter should be both rapid and adaptive, while the characteristics should be kept to a minimum while retaining as much of the SI as feasible. Even if the analogue cancellation is excellent enough to keep neither the LNA nor the ADC from being saturated, the digital cancellation must still cancel out the residuals quickly and accurately for full duplex to operate.

Aside from the MAC protocol, which enables FD communication, RSI has been a popular research topic among businesses and academics due to inadequate SI cancellation. A recent breakthrough in FD transceiver technology can reach a SI cancellation of 110 dB [4]. Even with a high Signal to Noise Ratio (SNR), a large contribution of RSI after the analogue and digital SI cancellation degrades system performance such as Symbol Error Rate (SER), throughput, and so on [19]. Cheng Li et al. investigated the outage probability of an FD relay system when RSI and

imperfect Channel State Information (CSI) were combined [20]. Nirmal et al. investigated Half Duplex (HD) and FD radio in two-way and two-hop communication in terms of degrees of freedom using a realistic residual SI model [21].

2.4 Modulation Techniques

Jiliang et al. [22]. investigated FD communication using the spatial modulation technique at the source and maximum probability detection at the destination. Bingqi Zhang and colleagues investigated FD communication in an optical wireless network using M-ary Pulse Amplitude Modulation (MPAM) [23]. In [23], the authors maximised the aggregate attainable rate of FD communication by taking into account the constellation signal level and its associated probability distribution. Abbas Koohian et al. suggested a superimposed signalling technique to decode the symbols in FD communication while taking the receiver's RSI into account [24].

2.5 Unique Contribution

To completely achieve FD communication, SI cancellation and RSI suppression are required. Traditionally, SI cancellation has been accomplished through antenna and analogue cancellation, followed by digital processing, which necessitates precise channel state information understanding (CSI). The FD communication was studied in the references [19], [20], [21] by suppressing the SI with complex SI mitigation hardware circuits. Some works, such as [22], [23], [24], looked at FD communication via the lens of spatial modulation techniques and interference signal constellation diagrams. However, in the first step, the aforementioned paper ([22], [23], [24]) required SI cancellation. This paper makes a unique addition by proposing a superimposed constellation-based FD MAC protocol that does not require CSI knowledge at the receiver. Ours is the first work that we are aware of that proposes and anal-

yses FD communication performance without cancelling SI. The suggested symbol decoding method successfully decodes the desired signal from the interfering signal while maintaining a low Symbol Error Rate (SER). The primary contributions of our proposed C-FD MAC protocol are listed below.

- We derive the SER, Packet Error Rate (PER) of C-FD MAC protocol for the case where node and AP transmit the symbols using BPSK and QPSK modulation, respectively, by considering the AWGN Channel.
- Simulation results have been shown and compared for different m-PSK modulation schemes.
- The analytical results for RTS collision probability and system throughput have been derived using the Markov chain model and validated against MATLAB-based simulation.
- effect of various system parameters such as (a) SNR, (b) different modulation Scheme, (c) maximum backoff, and (d) number of nodes in the network on the performance metrics have been studied.

Chapter 3

Proposed C-FD MAC Protocol

We divided this chapter into three sections and discussed three key aspects of our report in this chapter. The first section is about the system model, in which we define and explain the network model of FD communication. The packet symbols' encoding and decoding methods were further discussed. In the second section, we discussed the MAC protocol for the proposed model, including how RTS/CTS and packets are conveyed. In the final section, a symbol decoding algorithm for both symmetrical and asymmetrical links is provided.

3.1 Modeling of System

We consider a communication system with N nodes communicating with a single Access Point (AP) having FD capability. The nodes in the network may have FD or Half-duplex (HD) capability. The coexistence of FD and HD-enabled nodes in a WLAN can establish either a symmetrical or asymmetrical link, as shown in fig. 3.1. In the symmetrical link, node and AP ($node_1 \leftrightarrow AP$) simultaneously exchange

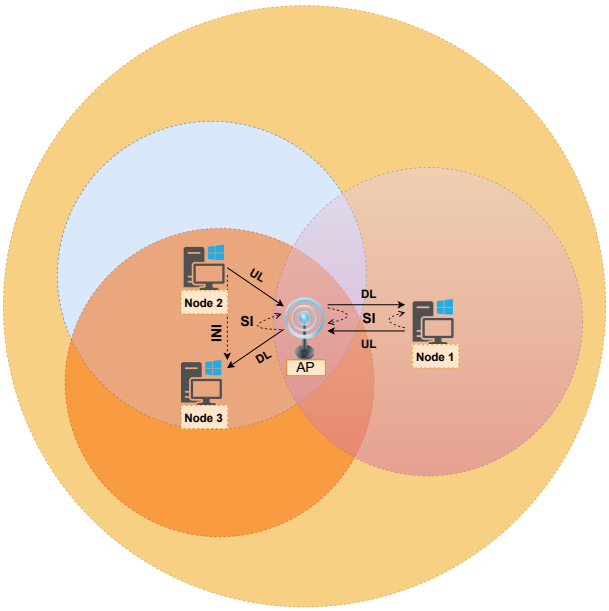

Figure 3.1: Network models for Full-Duplex Communication

packets over the same frequency. The symmetrical link can be possible only with FD capable node and AP, and both need to mitigate SI. In the asymmetric link ($node_1 \rightarrow AP \rightarrow node_3$), the node transmits a packet to AP, while the AP simultaneously transmits a packet to another node. The two-node ($node_2$ and $node_3$) that are in the range of each other and create an asymmetrical link ($node_2 \rightarrow AP \rightarrow node_3$), the Inter Node Interference (INI) along with SI are an important component that needs to be suppressed before decoding the desired packets [25]. If nodes are out of range ($node_1 \rightarrow AP \rightarrow node_3$), the only SI mitigation technique is required before decoding the desired packet at the AP. We consider the l^{th} packet of node n and AP consists of $L_{n,l}$ and $L_{AP,l}$ symbols respectively. We denotes the m^{th} symbol of packet l transmitted by node n and AP as $b_{n,l}[m]$ and $b_{AP,l}[m]$ respectively. Where $b_{\zeta,l}[m] \in \Theta_\zeta$, $\zeta \in \{n, AP\}$ and Θ_ζ be the set of finite symbols with χ_ζ symbols $a_{\zeta,i} \in \Theta_\zeta$, $1 \leq i \leq \chi_\zeta$. We assume symbol level synchronization have been maintained between each node and AP. In other words, node and AP transmit their symbol at the start of the symbol interval. We consider packet transmission between

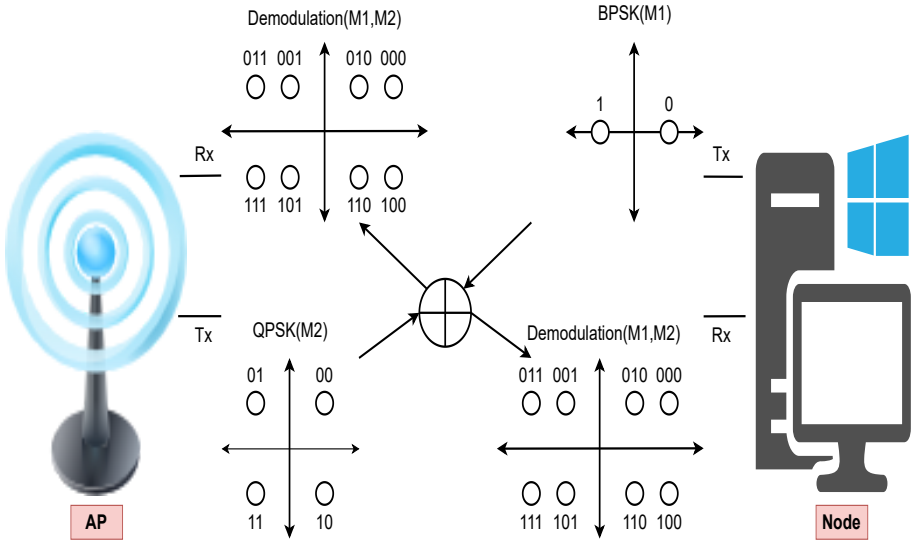

Figure 3.2: Example of C-FD MAC protocol

AP and nodes are affected by the Additive White Gaussian Noise (AWGN) channel having constant variance σ_N^2. We also assume the effect of inter symbol interference to be negligible. Fig. 3.2 shows an example of the C-FD MAC protocol, where AP and node transmit the symbols using Quadrature Phase Shift Keying (QPSK) and Binary Phase Shift Keying (BPSK) modulation, respectively. The interfered signal of two differently modulated symbols is received at the receiver end of the AP and node. The constellation diagram of the interfered signal can be used to decode the symbols at the AP and node.

3.2 C-FD MAC Protocol

The C-FD MAC protocol is described in detail in this section. The symbol decoding technique for both symmetrical and asymmetrical networks is described first, followed by the packet transmission protocol that supports FD communication.

The Request To Send (RTS) frame is sent by the nodes to initiate data packet transfer. The RTS frame is transmitted by the node using the IEEE 802.11 standard's default modulation technique. The AP responds with a Clear To Send (CTS) frame if the RTS sent by the node is successful, i.e. just one RTS transmission in a one-time slot. When a node's RTS transmission fails, it chooses a random backoff slot $BO \in [0, BO_{max} - 1]$ evenly, where BO_{max} is the maximum permitted backoff counter+, and sets the Retry sub-field (1 bit long) of the IEEE 802.11 RTS frame control field. In each time slot, the node's backoff counter is decremented by one unit. The node retries its RTS transmission if the backoff counter value hits 0. It's worth noting that the node retries packet transmission until it succeeds.

The MCS sub-field of the RTS frame is used by the nodes to tell the AP of their Modulation and Coding Scheme (MCS). The MCS is indicated differently in different editions of the IEEE standard. The HE header, which consists of HF SIG-A and HE SIG-B fields, can, for example, tell the AP about the node's MCS rate and modulation scheme in IEEE 802.11ay. The modulation scheme and coding rate of the packet transmitted by the node are stored in HE SIG-A. In response to the RTS delivered by the node, the AP informs its MCS through the CTS frame. If the AP has a packet for the same node, the symmetrical FD link is established; otherwise, an asymmetrical FD link can be established if the AP has a packet for a different node. The AP instructs the receiving node (say, node B) using the address field of the CTS to construct an asymmetrical link, and so the asymmetrical FD link can be established between Node A, AP, and Node B ($NodeA \rightarrow AP \rightarrow NodeB$).

3.3 C-FD MAC Symbol Decoding Algorithm

Following the C-FD MAC protocol, the AP and node may either create symmetrical link ($NodeA \leftrightarrow AP$) or asymmetrical link ($NodeA \rightarrow AP \rightarrow NodeB$). The symbol decoding algorithm for the symmetrical FD link has been shown in Algorithm 1. The node A and AP transmit a symbol $b_{A,l}[m]$ and $b_{AP,l}[m]$ of l^{th} packet in m^{th}

symbol interval respectively. Node A and AP stored the symbol transmitted by them and used it to decode the symbol from the received interfered signal $Y_l[m]$ at the receiver end of the device (Node A or AP). Based on the received signal $Y_l[m]$, node A and AP calculate the condition likelihood probability considering the constellation diagram of interfered received signal. The AP and node A estimate the symbol transmitted by node A and AP respectively as $\hat{b}_{A,l}$ and $\hat{b}_{AP,l}$. Note that $\hat{b}_{A,l}$ and $\hat{b}_{AP,l}$ are the estimated symbols correspond to maximum likelihood probability.

Algorithm 1 Symbol detection in symmetric FD link

Require: Transmit $b_{A,l}[m]$ and $b_{AP,l}[m]$
Ensure: Receiver end of node A and AP receive $Y_l[m]$
  if Decoding at AP **then**
    while $i \leq \chi_A$ **do**
      calculate $P_{AP,i} = P(a_{A,i}|Y_l[m], b_{AP,l}[m])$
    end while
  end if
  Find $k : P(a_{A,k}|Y_l[m], b_{AP,l}[m]) > P_{AP,i}\ \forall i \neq k$
  $\hat{b}_{A,l}[m] \leftarrow a_{A,k}$
  if Decoding at node A **then**
    while $j \leq \chi_{AP}$ **do**
      calculate $P_{A,j} = P(a_{AP,j}|Y_l[m], b_{A,l}[m])$
    end while
  end if
  Find $\kappa : P(a_{AP,\kappa}|Y_l[m], b_{A,l}[m]) > P_{A,j}\ \forall j \neq \kappa$
  $\hat{b}_{AP,l}[m] \leftarrow a_{AP,\kappa}$

For the asymmetrical link ($NodeA \rightarrow AP \rightarrow NodeB$), the AP knows the symbol transmitted by it and uses the transmitted symbol to decode the symbol transmitted by node A, as explained for the case of a symmetrical link. However, Node B is unaware of the symbol transmitted by both AP and Node A. Hence based on received signal $Y_l[m]$, and knowledge of modulation scheme used by the Node A and AP, Node B estimate the symbol transmitted by the AP. The symbol decoding algorithm for the case of asymmetrical link has been shown in Algorithm 2. Suppose

Algorithm 2 Symbol detection in asymmetric FD link

Require: Transmit $b_{A,l}[m]$ and $b_{AP,l}[m]$
Ensure: Receiver end of node B and AP receive $Y_l[m]$
  if Decoding at Node B with INI **then**
    while $i \leq \chi_{AP}$ **do**
      calculate $P_{B,i} = P(a_{AP,i}|Y_l[m], M_{AP}, M_A)$
    end while
  end if
  Find $k : P(a_{AP,k}|Y_l[m], M_{AP}, M_A) > P_{B,i}\ \forall i \neq k$
  $\hat{b}_{AP,l}[m] \leftarrow a_{AP,k}$
  if Decoding at Node B without INI **then**
    while $i \leq \chi_{AP}$ **do**
      calculate $P_{B,i} = P(a_{AP,i}|Y_l[m], M_{AP})$
    end while
  end if
  Find $k : P(a_{AP,k}|Y_l[m], M_{AP}) > P_{B,i}\ \forall i \neq k$
  $\hat{b}_{AP,l}[m] \leftarrow a_{AP,k}$
  if Decoding at AP **then**
    while $j \leq \chi_A$ **do**
      calculate $P_{AP,j} = P(a_{A,j}|Y_l[m], b_{AP,l}[m])$
    end while
  end if
  Find $\kappa : P(a_{A,\kappa}|Y_l[m], b_{AP,l}[m]) > P_{AP,j}\ \forall j \neq \kappa$
  $\hat{b}_{A,l}[m] \leftarrow a_{A,\kappa}$

Node A and Node B are in the range of each other, i.e., in the presence of INI, Node B estimate the symbol as $\hat{b}_{AP,l}$. The estimated symbol $\hat{b}_{AP,l}$ corresponds to the maximum likelihood probability given that Node A and AP use the modulation scheme M_A and M_{AP} respectively. If the Node A and Node B are out of range to each other, Node B estimate the symbol transmitted by the AP as $\hat{b}_{AP,l}$ based on the received signal $Y_l[m]$ and only the knowledge modulation scheme used by the modulation scheme of the AP M_{AP}.

Chapter 4

Analytical Derivations

The analytical results of the proposed C-FD MAC protocol's Symbol Error Rate (SER) and Packet Error Rate (PER) were derived in this section. We also used the discrete time Markov chain model to get analytical estimates for RTS collision probability and throughput.

4.1 Symbol Error Rate of proposed C-FD MAC protocol

The suggested C-FD MAC protocol's analytical results are significantly reliant on the modulation technique employed by the node and AP. The analytical results alter as the modulation scheme varies.

As a result, we investigate a scenario in which Node A and AP send a packet modulated using BPSK and QPSK, respectively. However, the analytical results for various Phase Shift Keying (PSK) modulation schemes can be obtained using a

similar approach.

The symbols are sent by Node A and AP with energy E_b and E_q, respectively. The set of symbols communicated by Node A and AP are $\Theta_A \in [0, 1]$ and $\Theta_{Ap} \in [00, 01, 10, 11]$, respectively. The constellation diagram for the superposition of BPSK and QPSK symbols is shown in Fig. 4.1a. In Fig. 4.1a, the first two bits of each symbol indicate the AP's symbol, while the last bit indicates the node's BPSK symbol.

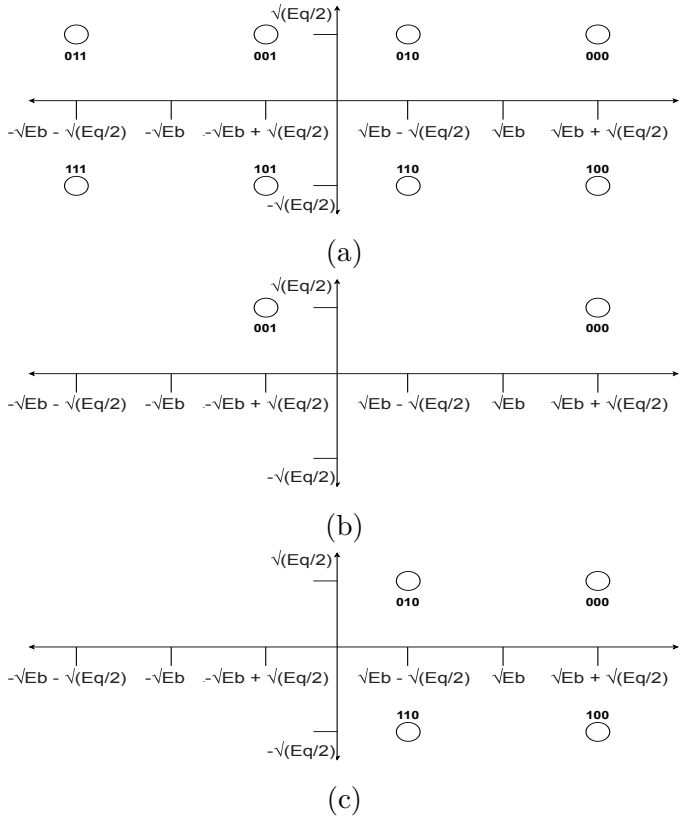

Figure 4.1: Constellation diagram for (a) interfered BPSK and QPSK symbols, (b) interfered signal given that symbol 00 was transmitted using QPSK modulation, (c) interfered signal given that symbol 0 was transmitted using BPSK modulation

4.1.1 SER at AP considering symmetrical link

Let $\gamma_{sym,AP}$ be the probability of bit error received at the AP in the case of a symmetrical link between Node A and AP. Note that the symbol is transmitted by AP and node A using the QPSK and BPSK modulation schemes, and AP must decode the BPSK symbol from the received interfering signal $Y_l[m]$. $\gamma_{sym,AP}$ can be written as follows:-

$$\begin{aligned}\gamma_{sym,AP} = P(00)\Big(P(0)P(1|0,00) + P(1)P(0|1,00)\Big)+\\ P(01)\Big(P(0)P(1|0,01) + P(1)P(0|1,01)\Big)+\\ P(10)\Big(P(0)P(1|0,10) + P(1)P(0|1,10)\Big)+\\ P(11)\Big(P(0)P(1|0,11) + P(1)P(0|1,11)\Big)\end{aligned} \tag{4.1.1}$$

where, $P(x)$ be the symbol transmission probability, and $P(\overline{b}_{A,l}[m]|b_{A,l}[m]|, b_{AP}[m])$ be the probability that AP decoded symbol as $\overline{b}_{A,l}[m]$ given that AP and Node A have transmitted symbol $b_{AP}[m]$ and $b_{A,l}[m]$ in the m^{th} bit interval. We consider the symbol transmitted by the Node A and AP from Θ_A and Θ_{AP} respectively are equi-probable, i.e., $P(0) = P(1) = 1/2$ for Node and $P(00) = P(01) = P(10) = P(11) = 1/4$ for the AP.

Given that the AP has transmitted symbol 00, the constellation diagram of interfered signal gets reduced to two point constellation diagram as shown in Fig. 4.1b. The point 000 and 001 in Fig. 4.1b represent the node has transmitted symbol 0 and 1 respectively given that AP has transmitted symbol 00. The probability that AP decoded the symbol transmitted by Node A as 0, given that Node A and AP have transmitted the symbols 1 and 00 respectively, i.e. $P(0|1,00)$ can be given as

$$P(0|1,00) = \frac{1}{\sqrt{2\pi\sigma_{N_0}^2}} \int_{\sqrt{E_q/2}}^{\infty} exp\Big(- \frac{(x + \sqrt{E_b} - \sqrt{E_q/2})^2}{2\sigma_{N_0}^2} \Big) dx \tag{4.1.2}$$

where, $\sigma_{N_0}^2$ be the variance of AWGN noise. Let us consider $Z = \frac{x+\sqrt{E_b}-\sqrt{E_q/2}}{\sqrt{2\sigma_{N_0}^2}}$. Substituting Z in eq. 4.1.2 and rearranging the terms, we gets $P(0|1,00)$ as

$$P(0|1,00) = \frac{1}{\sqrt{\pi}} \int_{\sqrt{E_b/\sigma_{N_0}^2}}^{\infty} exp(-Z^2) dZ = \frac{1}{2} erfc\left(\sqrt{\frac{E_b}{\sigma_{N_0}^2}}\right) \tag{4.1.3}$$

where $erfc(x)$ be the complementary error function evaluated for the value of x. Following the similar procedure for other transmitted symbol by the AP, we get

$$P(0|1,10) = P(0|1,11) = P(0|1,01) = \frac{1}{2} erfc\left(\sqrt{\frac{E_b}{\sigma_{N_0}^2}}\right) \tag{4.1.4}$$

Also due to symmetry of Gaussian curve around its mean value $P(0|1,00) = P(1|0,00)$. As a result, from eq. 4.1.1, 4.1.3, and 4.1.4, $\gamma_{symm,AP}$ can be be given as

$$\gamma_{symm,AP} = \frac{1}{2} erfc\left(\sqrt{\frac{E_b}{\sigma_{N_0}^2}}\right) \tag{4.1.5}$$

4.1.2 SER at the Node considering symmetrical link

Considering the symmetrical link, let $\gamma_{sym,node}$ denote the probability of symbol error received at the node. Note that Node A and AP transmit symbols using BPSK and QPSK modulation. Let P_{S_1,S_2} denote the confirmation probability of the symbol received by the node. In other word, confirmation probability represent the

successful symbol decoding probability. The transmitted bits S_1 and S_2 correspond to the QPSK symbol transmitted by the AP. P_{S_1,S_2} can be given as

$$P_{S_1,S_2} = P(X_1|S_1)P(X_2|S_2) \tag{4.1.6}$$

where $P(X_i|S_i)$ represents the probability of decoded bit as X_i given that bit S_i was transmitted by the AP. Given that Node A has transmitted the symbol 0, the constellation diagram of interfered signal gets reduce to four point constellation as shown in Fig. 4.1c. Considering the AWGN noise at the receiver, P_{S_1,S_2} can be given as

$$P_{S_1,S_2} = \prod_{k=1}^{2}\left(\frac{1}{\sqrt{2\pi\sigma_{N_0}^2}}\int_{\sqrt{E_b}}^{\infty} exp\left(-\frac{(x_k-\sqrt{E_b}-\sqrt{E_q/2})^2}{2\sigma_{N_0}^2}\right)dx_k\right) \tag{4.1.7}$$

Let $Z_k = \frac{x_i-\sqrt{E_b}-\sqrt{E_q/2}}{\sqrt{N_0}}$. Substituting Z_k in eq. 4.1.7 and rearranging the terms, we gets P_{S_1,S_2} as

$$\begin{aligned} P_{S_1,S_2} &= \prod_{k=1}^{2}\left(\frac{1}{\sqrt{\pi}}\int_{-\sqrt{E_q/2\sigma_{N_0}^2}}^{\infty} exp(-Z_k^2)dZ_k\right) \\ &= \left(1-\frac{1}{2}erfc\left(\sqrt{\frac{E_q}{2\sigma_{N_0}^2}}\right)\right)^2 \end{aligned} \tag{4.1.8}$$

Simplifying the eq. 4.1.8 by neglecting the higher power terms of $erfc(x)$ (higher

power term tends to 0), P_{S_1,S_2} can be rewritten as as

$$P_{S_1,S_2} = \left(1 - erfc\left(\sqrt{\frac{E_q}{2\sigma_{N_0}^2}}\right)\right) \tag{4.1.9}$$

From eq. 4.1.9 and eq. 4.1.10, the probability of bit error rate $\gamma_{sym,node}$ can be derived as

$$\gamma_{symm,node} = 1 - P_{S_1,S_2} = erfc\left(\sqrt{\frac{E_q}{2\sigma_{N_0}^2}}\right) \tag{4.1.10}$$

4.1.3 SER at the AP considering Asymmetrical link

The AP in the symmetrical and asymmetrical link knows the symbol transmitted by it m^{th} bit interval. Hence the derivation of SER at the AP in asymmetrical link will be similar to the similar to the symmetrical link as we have derived in section 4.1.1. Let $\gamma_{Asymm,AP}$ be the probability of bit error received at the AP. $\gamma_{Asymm,AP}$ can be written as

$$\gamma_{Asymm,AP} = \gamma_{symm,AP} = \frac{1}{2} erfc\left(\sqrt{\frac{E_b}{\sigma_{N_0}^2}}\right) \tag{4.1.11}$$

4.1.4 SER at the Node considering Asymmetrical link

Let $\gamma_{Asym,node}$ denotes the probability of symbol error at the node considering asymmetrical link. Node B has to decode the QPSK signal transmitted by the AP from the interfered received signal $Y_l[m]$. Note that, in an asymmetrical link Node B only has information about the modulation scheme used by the Node A and AP. The actual symbol transmitted by the Node A is unknown to the Node B. If the Node A and Node B are out of range to each other, Node B has knowledge of modulation scheme used by the AP. Hence, Node B have to compute the likelihood probability considering all the eight point of the constellation diagram show in Fig. 4.1a. Let

$\mathbb{P}_{S_1,S_2,S_3}$ be the confirmation probability of the symbol received at the Node B. The first two bits S_1 and S_2 represent the symbol transmitted by the AP, and the last bit S_3 represent the symbol transmitted by Node A. P_{S_1,S_2,S_3} can be given as

$$\mathbb{P}_{S_1,S_2,S_3} = P(X_1|S_1)P(X_2|S_2)P(X_3|S_3) \tag{4.1.12}$$

Where where $P(X_i|S_i)$ represents the probability of decoded bit as X_i given that bit S_i was transmitted by the AP. Considering the AWGN channel, eq. 4.1.12 can we written as

$$P_{S_1,S_2,S_3} = \prod_{k=1}^{3}\left(\frac{1}{\sqrt{2\pi\sigma_{N_0}}}\int_{\sqrt{E_b}}^{\infty} exp\left(-\frac{\left(x_k-\sqrt{E_b}-\sqrt{E_q/2}\right)^2}{2\sigma_{N_0}^2}\right)dx_k\right) \tag{4.1.13}$$

Let us consider $Z_k = \frac{x_k-\sqrt{E_b}-\sqrt{E_q/2}}{\sqrt{N_0}}$. Substituting Z_k in eq. 4.1.13 and rearranging the terms, we gets P_{S_1,S_2,S_3} as

$$\begin{aligned} P_{S_1,S_2,S_3} &= \prod_{k=1}^{3}\left(\frac{1}{\sqrt{\pi}}\int_{-\sqrt{E_q/2\sigma_{N_0}}}^{\infty} exp(-Z_k^2)dZ_k\right) \\ &= \left(1-\frac{1}{2}erfc\left(\sqrt{\frac{E_q}{2\sigma_{N_0}}}\right)\right)^3 \end{aligned}$$

Neglecting higher power term of $erfc(x)$ from eq. 4.1.4, the simplified expression of P_{S_1,S_2,S_3} can be written as

$$P_{S_1,S_2,S_3} = \left(1-\frac{3}{2}erfc\left(\sqrt{\frac{E_q}{2\sigma_{N_0}}}\right)\right) \tag{4.1.14}$$

The probability of bit error $\gamma_{Asymm,node}$ at the Node under asymmetrical link can be

given as

$$\gamma_{Asymm,node} = 1 - P_{S_1,S_2,S_3} = \frac{3}{2} erfc\left(\sqrt{\frac{E_q}{2\sigma_{N_0}}}\right) \tag{4.1.15}$$

4.2 Packet Error Rate of proposed C-FD MAC protocol

The n^{th} node and the AP transmit an l^{th} packet having $L_{n,l}$ and $L_{AP,l}$ symbols. A packet is successfully decoded if all of its symbols decoded correctly. Note that we have not incorporated the any Forward Error Correction (FEC) coding. We assume even if one symbol in the packet has been decoded incorrectly, packet is said to be corrupted. However, further incorporating FEC coding will further reduce the PER. Let $\Gamma_{\epsilon,\zeta}$, where $\epsilon \in [symm, asymm]$ and $\zeta \in [n, AP]$ denotes the PER without FEC coding at the node n and AP considering the symmetrical and asymmetrical link. $\Gamma_{\epsilon,\zeta}$ can be given as

$$\Gamma_{\epsilon,\zeta} = 1 - (1 - \gamma_{\epsilon,\zeta})^{L_{\zeta,l}} \tag{4.2.1}$$

4.3 RTS Collision Probability of proposed C-FD MAC protocol

The discrete time Markov chain for the backoff status of node has been shown in Fig. 4.2. Let $W \in [0, BO_{max}]$ denote the state representing backoff status of node at any given time slot. Let Υ denote the state transition matrix with element $\upsilon_{i,j}$ representing the state transition probability from state i to state j for the Markov chain shown in Fig. 4.2. $\upsilon_{i,j}$ can be written as

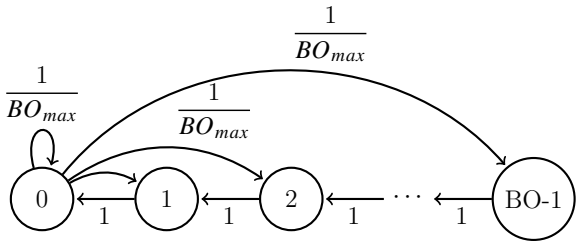

Figure 4.2: Markov chain for the backoff slot of node

$$\upsilon_{i,j} = \begin{cases} \frac{1}{BO_{max}} & i = 0,\ \ 0 \leq j \leq BO_{max} - 1 \\ 1 & \text{i} \neq 0, \quad j = i - 1 \\ 0 & otherwise \end{cases} \tag{4.3.1}$$

Let $\Lambda = \{\lambda_0, \lambda_0, ..., \lambda_{BO_{max}-1}\}$ denotes the steady state probability vector wherein λ_i represent the steady state probability of node being in state i. Λ can be calculated by solving steady state equation $\Lambda = \Lambda\Upsilon$ with subjected to $\sum_{i=0}^{BO_{max}-1} \lambda_i = 1$.

The steady state probability λ_0 indicate that the backoff counter value of the node is 0 and hence node is ready to transmit the RTS. Therefore λ_0 represent the steady state RTS transmission probability. If two or more nodes send the RTS in a time slot, the RTS gets collided. Let ψ denote the RTS collision probability. ψ can be given as

$$\psi = 1 - (1 - \lambda_0)^N - N\lambda_0(1 - \lambda_0)^{N-1} \tag{4.3.2}$$

4.4 Throughput of proposed C-FD MAC protocol

This sub-section derived the saturated throughput. We assume AP always have packet for transmission over asymmetrical or symmetrical FD link. Let $\aleph$ denote

the saturated throughput of C-FD MAC protocol. $\aleph$ can be given as

$$\aleph = \Phi\Big[2(1-\Gamma_{\epsilon,node})(1-\Gamma_{\epsilon,AP}) + (1-\Gamma_{\epsilon,AP})\Gamma_{\epsilon,node} + (1-\Gamma_{\epsilon,node})\Gamma_{\epsilon,AP}\Big] \quad (4.4.1)$$

where, $\epsilon \in \{Symm\ Asymm\}$. The first term in eq. 4.4.1 represent the packet transmission probability following the C-FD MAC protocol. Second term of eq. 4.4.1 represents the expected number of packet at the node and AP considering the symmetrical and asymmetrical link.

Chapter 5

Results and Discussion

We used MATLAB-based simulation to validate our analytical results in this part. To model the results, we used MATLAB's Communication Toolbox. At the AP and node, we consider a saturated traffic situation. Our model is validated by the excellent agreement between simulation and analytical data. Table reftab:my-table shows the simulation parameter that was used.

In this section, we validated our analytical results with MATLAB-based simulation. We utilized the Communication Toolbox in MATLAB to simulate the results. We consider a saturated traffic condition at the AP and node. The perfect match between simulation and analytical results validates our model. The simulation parameter used has been shown in Table 5.1.

Table 5.1: Parameter Used

Parameter	**value**
SNR(dB)	-2 - 15
N	10 - 200
BO_{max}	64,128,256
m-PSK	4,8,16,32,64
packet length	1500 Bytes
E_b	1 unit
E_q	1unit
$slot_{max}$	1,00,000

5.1 Symbol Error Rate

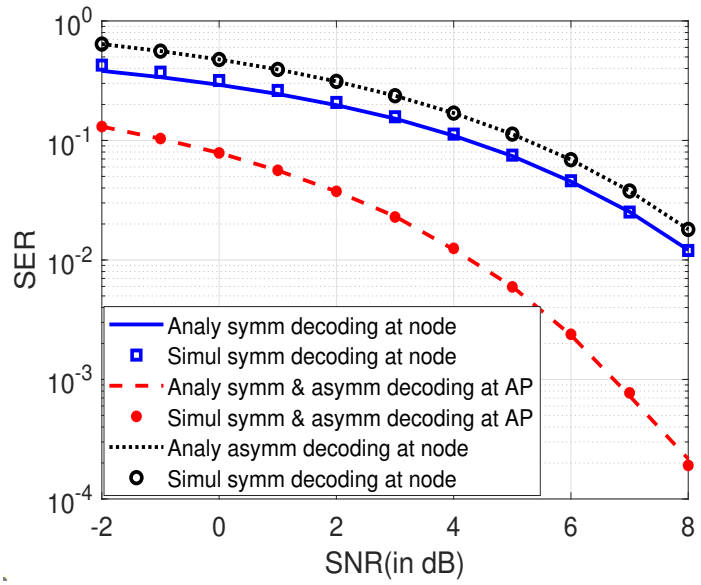

Figure 5.1: Symbol error rate at node and AP using BPSK and QPSK modulation respectively

Figure 5.1 shows the SER at the AP and node under symmetrical and asymmetrical links. Figure 5.1 illustrates that SER at the AP and node decreases as SNR increases. This is due to the fact that as SNR increases, symbol signal power compared to the noise power increases, which increases the likelihood probability of estimated symbol and aids the symbol decoding at the receiver. AP and node transmitting symbols using QPSK and BPSK modulation. Hence AP has to decode the BPSK symbols transmitted by the node, while the node has to decode QPSK symbols transmitted by the AP. Therefore SER at the node is lower than the SER at the AP. To decode the QPSK symbol transmitted by the AP, the node has to calculate likelihood probability with four points of the interfered constellation diagram, whereas to decode the BPSK symbol AP has likelihood probability with two points. Hence, the SER at the AP is lower than the SER at the node. Figure 5.1 also illustrates that SER at the node for the asymmetrical link is higher than the

symmetrical link. In the case of a symmetrical link, the node has knowledge about the transmitted symbols as well the modulation scheme used by the node and AP. On the other hand, in the asymmetrical link node only has knowledge about the modulation scheme used by the node (in the case of INI) and AP. Hence, the SER at the node is higher in an asymmetrical link than in a symmetrical link.

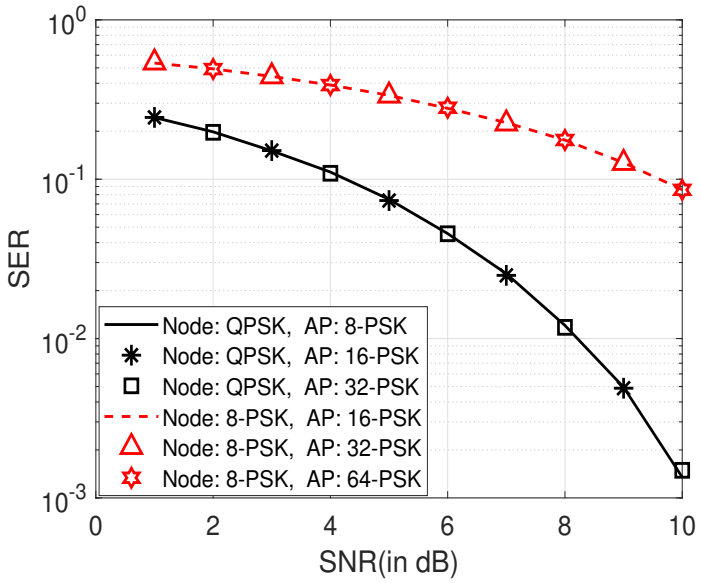

Figure 5.2: Symbol error rate at AP transmitting symbols with m-PSK modulation in symmetrical and asymmetrical link,

Figure 5.2 shows the SER as a function of SNR at the AP for the different modulation schemes used by the node and AP. Figure 5.2 illustrates that the SER at the AP depends only on the modulation scheme used by the node and is independent of the AP's modulation scheme. If the symbol is decoded at AP, as the modulation scheme used by the AP changes, only the points in the constellation diagram get translated, while the distance between the two points remains the same. Given that AP has used modulation scheme M_{AP}, the distance between the two points is the function of modulation scheme M_n used by the node n. Hence the SER at the AP is a function of M_n and independent of M_{AP}. Figure 5.2 also illustrate that SER at

the AP is higher if AP has to decode 8-PSK symbols compared to QPSK symbols transmitted by the node. As the node uses a higher modulation scheme, the points in the constellation diagram increase, and the distance between the points decreases, so SER at the AP increases.

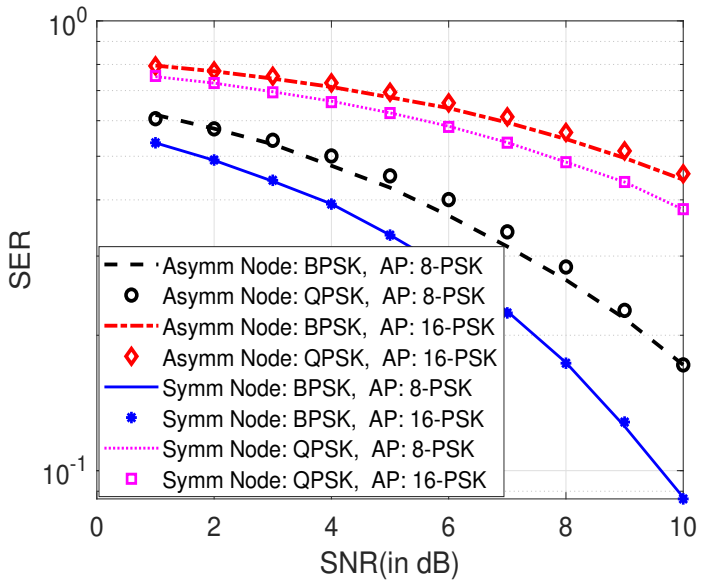

Figure 5.3: Symbol error rate at node different modulation scheme in symmetrical and asymmetrical link

Figure 5.3 shows the SER at the node for different modulation schemes used by the AP and the node. Following the similar trend as discussed in Fig. 5.2, SER at the node depends on the modulation scheme used by the AP and is independent of its own modulation scheme. Figure 5.2 also illustrates that as the higher modulation scheme used by the AP, SER at the node increases. The increase in SER with a higher modulation scheme has been explained in Fig. 5.2.

5.2 Packet Error Rate

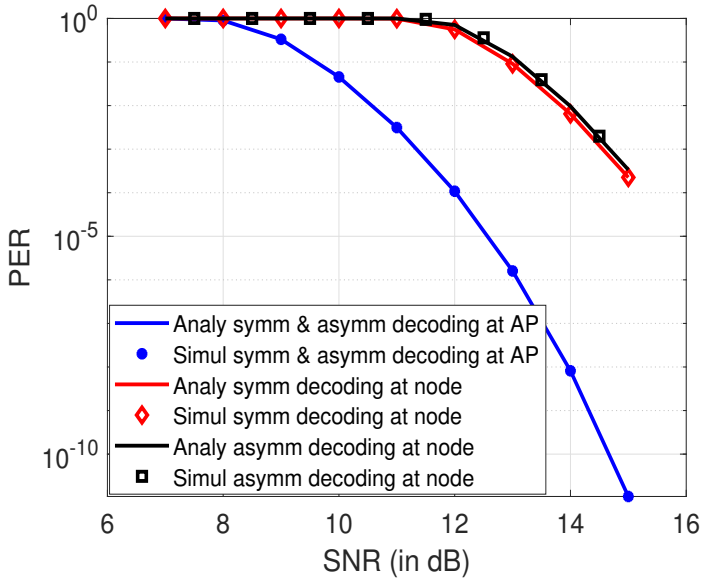

Figure 5.4: Packet Error Rate at the node and AP for symmetrical and asymmetrical link, L_{pkt} = 1500 Bytes

Figure 5.4 shows the PER at the AP and node transmitting symbols using QPSK and BPSK modulation. Figure 5.4 illustrate that PER at the node and AP decreases as SNR increases. The PER is a function of BER and as SNR increases the BER decreases as explained in Figure 5.1. Hence PER decreases with increase in SNR. Figure 5.4 also illustrate that PER at the AP is lower compared to the PER at the node. AP has to decode BPSK symbols transmitted by the node while node has to decode QPSK modulated symbols. As the modulation scheme used to encode symbols increase the BER also increase as explained in Figure 5.1. Hence PER increase.

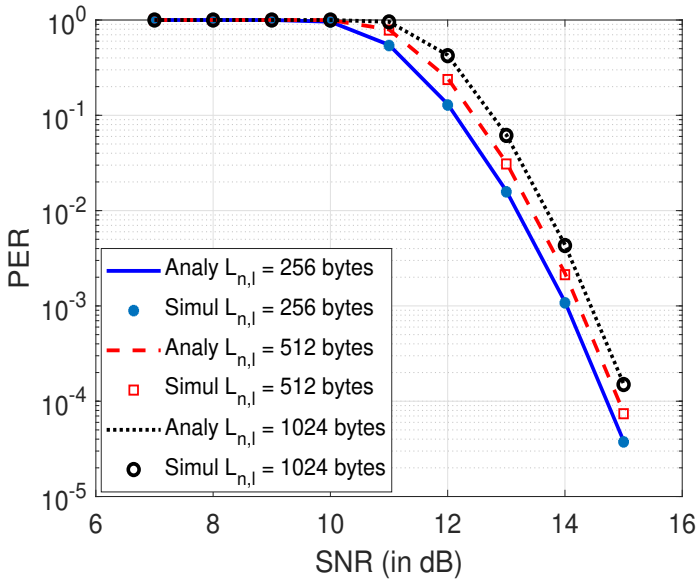

Figure 5.5: Packet Error Rate at the node for different packet length

Figure 5.5 shows the shows the PER at the node as a function of SNR for different packet length L_{pkt}. Figure 5.5 illustrate that for a given SNR PER decreases as packet length L_{pkt} increases. This is due to the fact that as the packet length L_{pkt} increases, the probability of simultaneously decoding all the symbol in it decreases which reduces the PER.

5.3 RTS Collision Probability

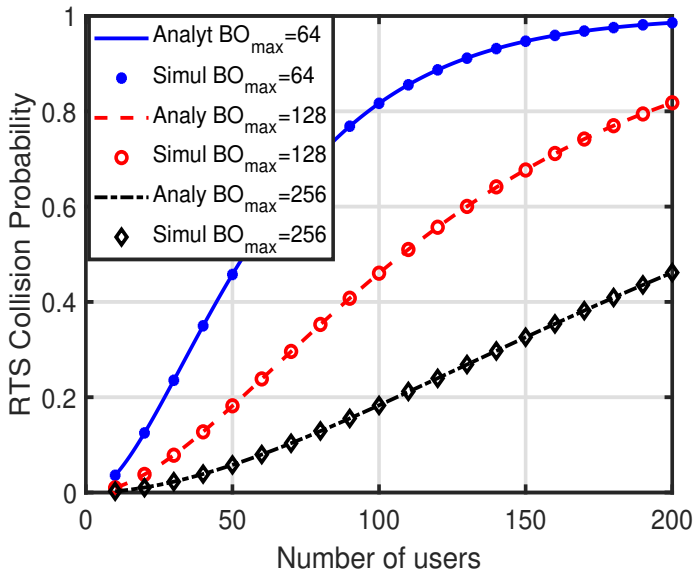

Figure 5.6: RTS collision Probability

Figure 5.6 shows the RTS collision probability as a function of number of nodes in the network for different BO_{max}. Figure 5.6 illustrate that RTS collision probability with increase in the number of nodes in the network for given BO_{max}. As the number of nodes in the networks increases, the probability that more then one node transmits the RTS in given slot increases, and hence RTS collision probability increases. Figure 5.6 also illustrate that, for a given number of nodes in the network, RTS collision probability decreases with increase in BO_{max}. This is due to the fact that, with increase in BO_{max} nodes can randomly select larger backoff counter value. The RTS transmission probability by the node in a given slot decreases as node takes the larger backoff counter value, and hence RTS collision probability decreases.

5.4 Saturated Throughput

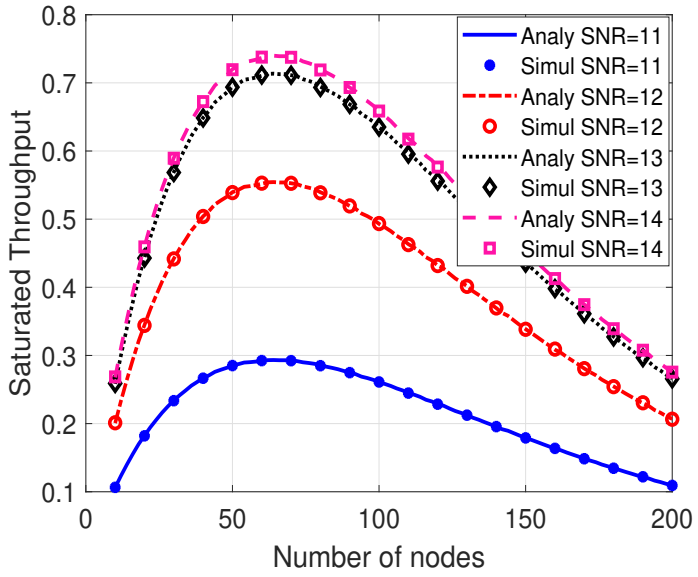

Figure 5.7: Throughput in case of Symmetrical link when BO_{max}=128

Figure 5.7 shows the saturated throughput $\aleph$ as function of number of node for $BO_{max} = 128$ considering the symmetrical link. Figure 5.7 illustrate that for a given SNR, saturated throughput $\aleph$ increases with an increase in the number of nodes and reaches the peak value $\aleph_p$. After the peak value $\aleph_p$, saturated throughput decreases with an increase in the number of node. This is because with fewer nodes in the network, the RTS transmission probability of the node is less, and hence saturated throughput increases with an increase in the number of nodes. After throughput reaches the peak value, the number of nodes attempting RTS transmission increases. With the increase in RTS attempt made by the node, collision increase, and hence throughput decreases. Figure 5.7 also illustrates that for a given number of nodes and BO_{max} saturated throughput increase with the increase in SNR. With the increase in SNR, PER decreases, as explained in Figure 5.4. As the PER decreases with increase in SNR, the saturated throughput increases.

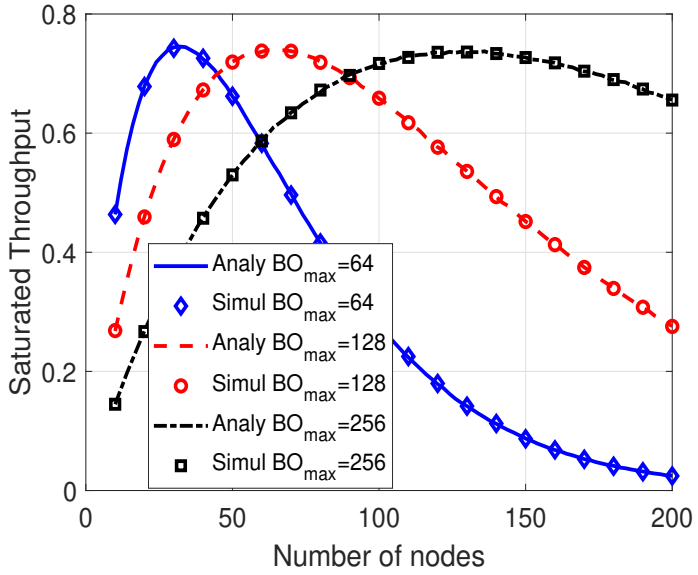

Figure 5.8: Throughput in case of Symmetrical link when SNR=14dB

Figure 5.8 shows the saturated throughput as a function of the number of nodes for different values of BO_{max} for the case of a symmetrical link. Figure 5.8 illustrates that the peak value of the saturated throughput shifts to the higher value of the number of nodes as BO_{max} increases. As BO_{max} increases, the RTS collision probability reduces, as explained in Figure 5.6, and hence network requires more nodes to achieve the peak throughput.

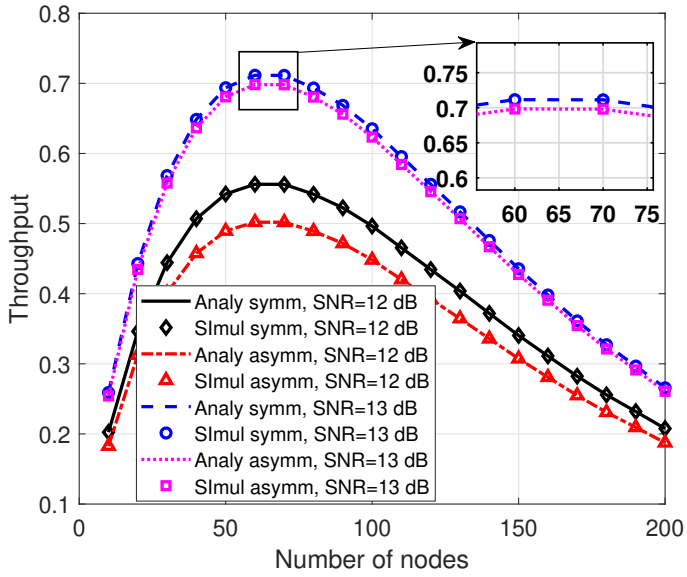

Figure 5.9: Throughput in case of Symmetrical and Asymmetrical link when BO_{max}=128

Figure 5.9 compared the saturated throughput for the case of symmetrical and asymmetrical link for $BO_{max} = 128$. Figure 5.9 illustrate that for a given SNR and number of node in the network, the saturated throughput for the symmetrical link is higher compared to the asymmetrical link. This is due to the fact that the SER for the asymmetrical is higher compared to the symmetrical link, as explained in figure 5.1. Hence the saturated throughput is less in asymmetrical links compared to symmetrical links.

Chapter 6

Conclusion

This report proposed an efficient symbol decoding technique for Full-Duplex (FD) communication that does not suppress SI at the receiver. We investigate both symmetrical and asymmetrical networks and offer an FD MAC protocol that is both efficient and effective. In the presence of SI, the proposed FD MAC technique uses interfering signal power constellation mapping and likelihood probability to estimate the transmitted symbol. Even in the case of asymmetrical link when nodes are in same range and forming inter node interference (INI) then also this technique work for decoding the transmitted symbol without suppressing INI. We used simulation to validate our analytical conclusions for symbol error rate, packet error rate, RTS collision probability, and saturated throughput. The proposed FD MAC protocol can achieve twice the throughput compared to half-duplex (HD) communication. We didn't sacrifice Symbol error rate to achieve the double throughput, which implies that the Symbol error rate is the same for both FD and HD communication.

Bibliography

[1] A. H. Gazestani, S. A. Ghorashi, B. Mousavinasab, and M. Shikh-Bahaei, "A survey on implementation and applications of full duplex wireless communications," *Physical Communication*, vol. 34, pp. 121–134, 2019.

[2] Z. Zhang, K. Long, A. V. Vasilakos, and L. Hanzo, "Full-duplex wireless communications: Challenges, solutions, and future research directions," *Proceedings of the IEEE*, vol. 104, no. 7, pp. 1369–1409, 2016.

[3] K. E. Kolodziej, B. T. Perry, and J. S. Herd, "In-band full-duplex technology: Techniques and systems survey," *IEEE Transactions on Microwave Theory and Techniques*, vol. 67, no. 7, pp. 3025–3041, 2019.

[4] B. C. Nguyen, T. M. Hoang, X. N. Tran, T. Kim *et al.*, "Impacts of imperfect csi and transceiver hardware noise on the performance of full-duplex df relay system with multi-antenna terminals over nakagami-m fading channels," *IEEE Transactions on Communications*, vol. 69, no. 10, pp. 7094–7107, 2021.

[5] T. Chen, S. Garikapati, A. Nagulu, A. Gaonkar, M. Kohli, I. Kadota, H. Krishnaswamy, and G. Zussman, "A survey and quantitative evaluation of integrated circuit-based antenna interfaces and self-interference cancellers for full-duplex," *IEEE Open Journal of the Communications Society*, vol. 2, pp. 1753–1776, 2021.

[6] C. D. Nwankwo, L. Zhang, A. Quddus, M. A. Imran, and R. Tafazolli, "A survey of self-interference management techniques for single frequency full duplex systems," *IEEE Access*, vol. 6, pp. 30 242–30 268, 2017.

[7] K. Yang, H. Cui, L. Song, and Y. Li, "Efficient full-duplex relaying with joint antenna-relay selection and self-interference suppression," *IEEE Transactions on Wireless Communications*, vol. 14, no. 7, pp. 3991–4005, 2015.

[8] P. K. Singya, P. Shaik, N. Kumar, V. Bhatia, and M.-S. Alouini, "A survey on higher-order qam constellations: Technical challenges, recent advances, and future trends," *IEEE Open Journal of the Communications Society*, vol. 2, pp. 617–655, 2021.

[9] T. Cover, "Broadcast channels," *IEEE Transactions on Information Theory*, vol. 18, no. 1, pp. 2–14, 1972.

[10] R. Zhang and L. Hanzo, "A unified treatment of superposition coding aided communications: Theory and practice," *IEEE communications surveys & tutorials*, vol. 13, no. 3, pp. 503–520, 2010.

[11] H. Ma, G. Cai, Y. Fang, P. Chen, and G. Chen, "Design of a superposition coding ppm-dcsk system for downlink multi-user transmission," *IEEE Transactions on Vehicular Technology*, vol. 69, no. 2, pp. 1666–1678, 2019.

[12] K. Chung, "Correlated superposition coding: Lossless two-user noma implementation without sic under user-fairness," *IEEE Wireless Communications Letters*, vol. 10, no. 9, pp. 1999–2003, 2021.

[13] D. Kim, H. Lee, and D. Hong, "A survey of in-band full-duplex transmission: From the perspective of phy and mac layers," *IEEE Communications Surveys & Tutorials*, vol. 17, no. 4, pp. 2017–2046, 2015.

[14] M. Amin, M. Hossain, M. Atiquzzaman *et al.*, "In-band full duplex wireless lans: Medium access control protocols, design issues and their challenges," *Information*, vol. 11, no. 4, p. 216, 2020.

[15] R. Rukaiya, M. U. Farooq, S. A. Khan, F. Hussain, and A. Akhunzada, "Cffd-mac: A hybrid mac for collision free full-duplex communication in wireless ad-hoc networks," *IEEE Access*, vol. 9, pp. 35 584–35 598, 2021.

[16] R. Kiran, N. B. Mehta, and J. Thomas, "Design and network topology-specific renewal-theoretic analysis of a mac protocol for asymmetric full-duplex wlans," *IEEE Transactions on Communications*, vol. 67, no. 12, pp. 8532–8544, 2019.

[17] J. Hu, B. Di, Y. Liao, K. Bian, and L. Song, "Hybrid mac protocol design and optimization for full duplex wi-fi networks," *IEEE Transactions on Wireless Communications*, vol. 17, no. 6, pp. 3615–3630, 2018.

[18] M. O. Al-Kadri, A. Aijaz, and A. Nallanathan, "An energy-efficient full-duplex mac protocol for distributed wireless networks," *IEEE Wireless Communications Letters*, vol. 5, no. 1, pp. 44–47, 2015.

[19] B. C. Nguyen, X. N. Tran *et al.*, "Transmit antenna selection for full-duplex spatial modulation multiple-input multiple-output system," *IEEE Systems Journal*, vol. 14, no. 4, pp. 4777–4785, 2020.

[20] C. Li, H. Wang, Y. Yao, Z. Chen, X. Li, and S. Zhang, "Outage performance of the full-duplex two-way df relay system under imperfect csi," *IEEE Access*, vol. 5, pp. 5425–5435, 2017.

[21] N. V. Shende, Ö. Gürbüz, and E. Erkip, "Half-duplex or full-duplex communications: Degrees of freedom analysis under self-interference," *IEEE Transactions on Wireless Communications*, vol. 17, no. 2, pp. 1081–1093, 2017.

[22] J. Zhang, Q. Li, K. J. Kim, Y. Wang, X. Ge, and J. Zhang, "On the performance of full-duplex two-way relay channels with spatial modulation," *IEEE Transactions on Communications*, vol. 64, no. 12, pp. 4966–4982, 2016.

[23] B. Zhang, C. Gong, S. Li, and Z. Xu, "Constellation design for led-based full-duplex vlc," in *2018 IEEE Global Conference on Signal and Information Processing (GlobalSIP)*. IEEE, 2018, pp. 186–190.

[24] A. Koohian, H. Mehrpouyan, A. A. Nasir, S. Durrani, and S. D. Blostein, "Residual self-interference cancellation and data detection in full-duplex communication systems," in *2017 IEEE International Conference on Communications (ICC)*. IEEE, 2017, pp. 1–6.

[25] L. H. Vu, R. Mareta, and J.-H. Yun, "Full-duplex wireless lan incorporating successive interference cancellation," *IEEE Transactions on Vehicular Technology*, vol. 70, no. 10, pp. 10 293–10 307, 2021.